Journal of Materials Chemistry C

Advantages of naphthalene as building block for organic solid state laser dyes: Smaller energy gaps and enhanced stability

Journal:	*Journal of Materials Chemistry C*
Manuscript ID	TC-ART-11-2020-005387.R1
Article Type:	Paper
Date Submitted by the Author:	25-Jan-2021
Complete List of Authors:	Oyama, Yuya ; Kyushu University, Center for Organic Photonics and Electronics Research (OPERA) Mamada, Masashi; Kyushu University, Center for Organic Photonics and Electronics Research (OPERA) Kondo, Akihiro; NIPPON SHIZAI CO., LTD., R&D Center Adachi, Chihaya; Kyushu University, Center for Organic Photonics and Electronics Research (OPERA)

ARTICLE

Advantages of naphthalene as building block for organic solid state laser dyes: Smaller energy gaps and enhanced stability

Received 00th January 20xx,
Accepted 00th January 20xx

DOI: 10.1039/x0xx00000x

Yuya Oyama,[ab] Masashi Mamada,*[abc] Akihiro Kondo,*[d] and Chihaya Adachi*[abce]

Organic laser dyes exhibiting very low amplified spontaneous emission (ASE) thresholds in green and yellow region were developed based on a stilbene structure which is often used for the blue laser molecules. Although the thresholds are generally increased with decreasing the energy levels of molecules, the introduction of a naphthalene unit can shift the emission colors without sacrificing optical properties. In particular, the suppression of the concentration quenching by naphthalene moieties resulted in high radiative decay rate constants and low ASE thresholds in the neat films. In addition, the photo- and thermal-stabilities of the naphthalene derivatives were improved compared to those of the corresponding phenylene derivatives. This study demonstrates a simple and effective molecular design for developing green and yellow laser dyes by a small modification from the standard blue emitters.

1. Introduction

Organic semiconductor laser diodes (OSLDs) have attracted increasing attention since the demonstration of lasing from an organic semiconductor device in 2019.[1] The device structure of OSLDs is similar to that of organic light-emitting diodes (OLEDs) with organic thin-films between two electrodes.[2] Therefore, OSLDs have the advantages such as surface emission, lightweight, flexible, color tunable and low cost production, and can be used for high resolution displays, analytical light sources, and sensors. However, the current OSLD is in the early stage of research and development, requiring significant improvement of its performances according to the OLED experience.

The development of new materials has still been active continuously for OLEDs since the fine-tuning of molecular structures steadily improves device performances.[3] Thus, organic semiconductor laser dyes, which fundamentally control laser properties as well as semiconducting properties, still need to be widely investigated. After the first report of lasing from organic dyes in solution in 1966, many chemical structures for organic laser media have been developed.[4] In terms of laser and amplified spontaneous emission (ASE) thresholds, E_{th}^{laser} and E_{th}^{ASE}, respectively, which are critical parameters for laser oscillation, some important classes of compounds have been identified to show low thresholds; Rhodamine,[5] pyrromethene,[6] DCM dyes (~1.2 μJ cm^{-2}),[7] coumarin dyes (~0.8 μJ cm^{-2}),[8] DABNA (1.6 μJ cm^{-2}),[9] excited-state intramolecular proton-transfer (ESIPT) materials (~1 μJ cm^{-2}),[10] phenylene oligomers (~0.09 μJ cm^{-2}),[11] phenylene-thienylene oligomers (1.8 μJ cm^{-2}),[12] and stilbene derivatives (~0.1 μJ cm^{-2}),[13,14] for small molecules, and polyfluorene (~0.3 μJ cm^{-2}),[15] polyphenylene vinylene derivatives (~0.02 μJ cm^{-2}),[16] and fluorene-benzothiadiazole copolymer (~2.7 μJ cm^{-2}),[17] for polymers. Meanwhile, a variety of novel organic semiconducting materials having the additional functions such as photoconduction and light emission have also been comprehensively developed for electrophotography and OLED applications. One most typical example of the organic semiconductors is aromatic amines, enabling the efficient hole injection and transport even at very high current density over 1 A cm^{-2}.[18] Since organic amines could also be a highly efficient emitter, many derivatives have widely been used in organic lasers.

In this study, we characterized optical properties of a diphenylamine incorporated distyrylbenzene derivative **1** and its analogues **2** and **3** (Fig. 1). The compound **1** has been used for organic photoconductors (OPCs),[19] and the laser properties for a very similar compound with the same π-conjugation structure (BSB3) were already reported.[13] Further, with keeping the scaffold of compound **1**, naphthalene moiety was introduced at the styryl unit in compounds **2** and **3** to extend the π-conjugation for red-shifting the emission spectra, and modulating stilbene's optoelectronic properties.[20] The stilbene derivatives are known to undergo *cis-trans* isomerization upon photoexcitation or at high temperature. This feature may relate

[a] Center for Organic Photonics and Electronics Research (OPERA), Kyushu University, Fukuoka 819-0395, Japan, E-mail: mamada@opera.kyushu-u.ac.jp; adachi@cstf.kyushu-u.ac.jp
[b] JST, ERATO, Adachi Molecular Exciton Engineering Project c/o Center for Organic Photonics and Electronics Research (OPERA), Kyushu University, Nishi, Fukuoka 819-0395, Japan
[c] Academia-Industry Molecular Systems for Devices Research and Education Center (AIMS), Kyushu University, Nishi, Fukuoka 819-0395, Japan
[d] R &D Center, NIPPON SHIZAI CO., LTD. 923-2, Touendo, Aisho-cho, Echi-gun, Shiga, 529-1325, Japan, E-mail: a-kondo@nippon-shizai.com
[e] International Institute for Carbon Neutral Energy Research (WPI-I2CNER), Kyushu University, Nishi, Fukuoka 819-0395, Japan

† Electronic supplementary information (ESI) available: Characterization, computational, photophysical, electrochemical, thin-film analysis, ASE and stability data. For ESI, see DOI: 10.1039/

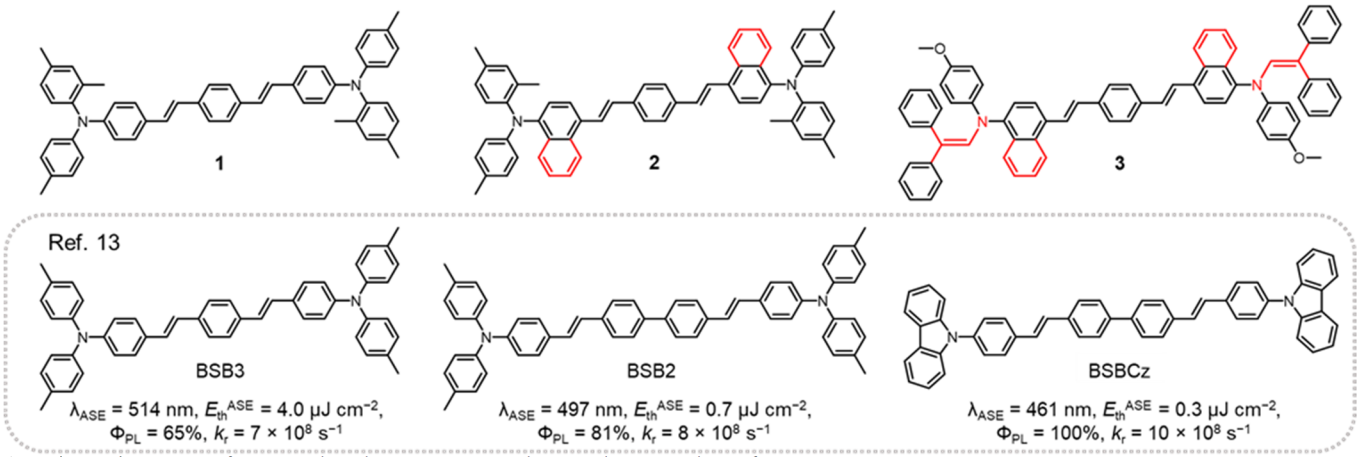

Fig. 1 Chemical structures of compounds under investigation and reported compounds in ref. 13.

to the degradation of the molecules according to our previous investigation for 4,4'-bis[(*N*-carbazole)styryl]biphenyl (BSBCz).[21] Since the extension of π-conjugation strongly affects the excited states dynamics of stilbene, the comparison of compounds **1** and **2** would give insights into optoelectronic properties of laser dyes. In addition, for exploring the possibility of modification of aryl amine structures, the enamine units introduced in compound **3** would afford further improvement based on the extension of π-conjugation.

2. Experimental

materials

The laser dyes **1**, **2** and **3** were supplied from NIPPON SHIZAI CO., LTD. and purified by column chromatography over silica gel using DCM as eluent, and characterized by ^{1}H and ^{13}C NMR spectra and elemental analysis. Their evaporation and decomposition temperatures were evaluated by thermogravimetric (TG) analysis at 1 and 10^5 Pa, respectively, and the melting points were evaluated by differential thermal analysis (DTA).

Compound **1** was obtained as a yellow solid. Mp: 200.6–201.8 °C. ^{1}H NMR (500 MHz, $CDCl_3$): δ/ppm 7.44 (s, 4H), 7.32 (d, *J* = 8.5 Hz, 4H), 6.99–7.07 (m, 12H), 6.91–6.96 (m, 6H), 6.87 (d, *J* = 8.5 Hz, 4H), 2.35 (s, 6H), 2.30 (s, 6H), 2.02 (s, 6H). ^{13}C NMR (125 MHz, $CDCl_3$): δ/ppm 147.6, 144.7, 142.7, 136.8, 136.3, 135.9, 132.5, 131.7, 129.8, 129.7, 129.4, 128.2, 128.1, 127.3, 126.6, 125.8, 122.7, 120.2, 21.2, 20.9, 18.6. Anal. calcd. for $C_{52}H_{48}N_2$: C 89.10, H 6.90, N 4.00; found: C 89.11, H 6.71, N 4.01.

Compound **2** was obtained as a yellow solid. Mp: 260.0–261.7 °C. ^{1}H NMR (500 MHz, $CDCl_3$): δ/ppm 8.25 (d, *J* = 8.2 Hz, 2H), 7.96 (t, *J* = 9.0, 3H), 7.90 (s, 1H), 7.67 (d, *J* = 7.3 Hz, 2H), 7.62 (s, 4H), 7.46–7.52 (m, 2H), 7.36 (t, *J* = 9.0, 2H), 7.14 (s, 1H), 7.08–7.14 (m, 3H), 7.05 (s, 2H), 6.91–6.98 (m, 8H), 6.64 (s, 4H), 2.32 (s, 6H), 2.27 (s, 6H), 2.04 (s, 6H). ^{13}C NMR (125 MHz, $CDCl_3$): δ/ppm 147.6, 145.0, 137.3, 134.6, 134.5, 133.0, 132.5, 131.7, 130.6, 130.1, 129.6, 127.7, 127.5, 127.1, 126.2, 125.8, 125.7, 125.5, 124.3, 124.1, 124.1, 120.8, 21.1, 20.8, 19.1. Anal. calcd for $C_{60}H_{52}N_2$: C 89.96, H 6.54, N 3.50; found: C 89.97, H 6.64, N 3.35.

Compound **3** was obtained as an orange solid. Mp: 137.4–138.9 °C. ^{1}H NMR (500 MHz, $CDCl_3$): δ/ppm 8.06 (d, *J* = 8.5 Hz, 2H), 7.78–7.82 (m, 3H), 7.76 (s, 1H), 7.61 (s, 4H), 7.39–7.44 (m, 4H), 7.32 (t, *J* = 7.6, 2H), 7.16–7.26 (m, 10H), 7.12 (t, *J* = 7.9, 2H), 7.07 (s, 2H), 7.02 (s, 1H), 6.99 (s, 1H), 6.89 (d, *J* = 8.9 Hz, 4H), 6.76 (d, *J* = 8.9 Hz, 4H), 6.63–6.73 (m, 10H), 3.76 (s, 6H). ^{13}C NMR (125 MHz, $CDCl_3$): δ/ppm 155.1, 142.3, 138.7, 133.0, 132.5, 132.5, 130.7, 130.1, 129.7, 128.3, 127.1, 127.0, 126.2, 125.9, 125.8, 125.7, 125.6, 125.5, 123.5, 120.8, 114.5, 55.8. Anal. calcd for $C_{72}H_{56}N_2$: C 88.13, H 5.75, N 2.85; found: C 87.99, H 5.69, N 2.87.

Fabrication of thin films

The substrates were washed by ultrasonic cleaning with acetone and isopropanol, followed by UV/ozone treatment for 15 min. For the preparation of the neat films, the emitter compounds (0.8, 1.0, and 1.2 wt%) were dissolved in chloroform and warmed-up to 50 °C and spin-coated at a speed of 1000 rpm for 60 s at 50 °C. For the doped films, the emitter compounds (6 and 8-wt%-doped) in the host material, 4,4'-*N*,*N*-dicarbazole-biphenyl (CBP) were dissolved in chlorobenzene (2.7 wt%), then the solution was warmed-up to 110 °C, and filtered, and spin-coated at a speed of 1000 rpm for 60 s at 110 °C.

ASE characteristics

The ASE properties were measured under nitrogen atmosphere in order to prevent the degradation of organic thin films. The excitation light was a nitrogen gas laser at an excitation wavelength of 337 nm. The output emission from the edge of the sample was collected by the detector (PMA-12) while sweeping the excitation light power. The ASE threshold (E_{th}^{ASE}) was determined from the non-linear changes of the emission intensity plotted against the excitation light intensity. The reproducibility was guaranteed by measuring the same samples more than five times.

Evaluation of photo-stability

The photo-stability of **1**, **2**, **3** and BSBCz in the neat films was evaluated by using a CW laser diode with an excitation wavelength of 355 nm. The exciton density was the same for all

samples (120 mW cm^{-2}) by adjusting the film thickness. The changes of emission intensity were monitored using a PMA-12.

DFT calculation

The molecular orbital calculation was performed by Gaussian 16. The ground state structure is optimized at the B3LYP/6-31+G(d,p) level. The time-dependent density functional theory (TD-DFT) calculations were conducted at the B3LYP/6-31+G(d,p).

3. Results and discussion

The solubilities of **1**, **2** and **3** in chloroform were ca. 25.8, 7.1 and 9.6 wt%, respectively, and the thin films with several hundred nanometers thickness could be easily fabricated by solution processes such as spin-coating. The introduction of naphthalene units slightly decreased the solubility in chloroform, while the enamine moieties in **3** enhanced the solubility.

Although the films were prepared using spin-coating in this work, vacuum evaporation capability was also investigated. In addition, thermal stability of materials is an important property to improve device durability. Fig. S1a shows thermogravimetry (TG) at 10^5 Pa, which generally indicates decomposition temperature of compounds. The 5% weight loss temperatures (T_d) are almost similar for three compounds, which suggested that the double bonds in the stilbene moiety or C—N single bonds causes initial decomposition. Therefore, the introduction of naphthalene units seems to have less impact on the thermal stability. Note that T_d cannot represent all decomposition paths including isomerization and rearrangement, therefore the small decomposition might occur at lower temperature than T_d. Further, the TG characteristics at 1 Pa in Fig. S1b shows the loss of weights; 5% loss temperature can be related to the evaporation (sublimation) temperature (T_{evap} (T_{sub})). The compound should be able to evaporate or sublime when the T_d is much higher than T_{evap} or T_{sub}. For example, BSBCz showed T_d at 478 °C (Fig. S1c) and T_{sub} at 324 °C (Fig. S1d). Nevertheless, BSBCz undergoes a large volume of decomposition at ~360 °C during standard sublimation at >10^{-2} Pa, and *cis*-isomerization at a slightly lower temperature of ~320 °C during vacuum deposition at a low pressure of 10^{-4} Pa.[21] Similarly, although compound **1** showed a large difference between T_d of 431 °C and T_{evap} of 284 °C, some decomposition products were found in the NMR spectra for the powder of **1** after heating at 300 °C (Fig. S2). The decomposition for compound **2** with heating at 300 °C was quite small, suggesting that the naphthalene units potentially increase the stability of the styryl structures. Although the vacuum deposition for fabricating the thin film of compound **2** might be possible in the deposition chamber with the high vacuum level, compounds **1** and **3** are unsuitable for vacuum evaporation processes.

Fig. 2 shows the absorption and photoluminescence (PL) spectra in toluene, in doped films with a CBP host, and neat films. The emission maxima of **1** are 460 and 488 nm in solution, and 490 and 518 nm in the neat films (Table 1), which are 40 nm red-shifted from those of BSBCz because of stronger donor nature of diphenyl amine compared to carbazole.[21] The emission maxima for compounds **2** and **3** were further red-shifted and appeared at green region. In fact, the energy gaps between the highest occupied molecular orbital (HOMO) and the lowest unoccupied molecular orbital (LUMO) estimated by electrochemical measurements (Fig. S3–S4 and Table S1) and the density functional theory (DFT), and the excitation energies estimated by the time-dependent (TD)-DFT calculations are decreasing in order from **1** to **3** (Fig. S5 and Table S2). The PL quantum yields (Φ_{PL}) and the radiative rate constant (k_r) of **1** and **2** in solution are comparable although those of **3** are relatively low. Interestingly, the Φ_{PL} and the k_r of **2** in the doped and neat films were higher than those of **1**, suggesting

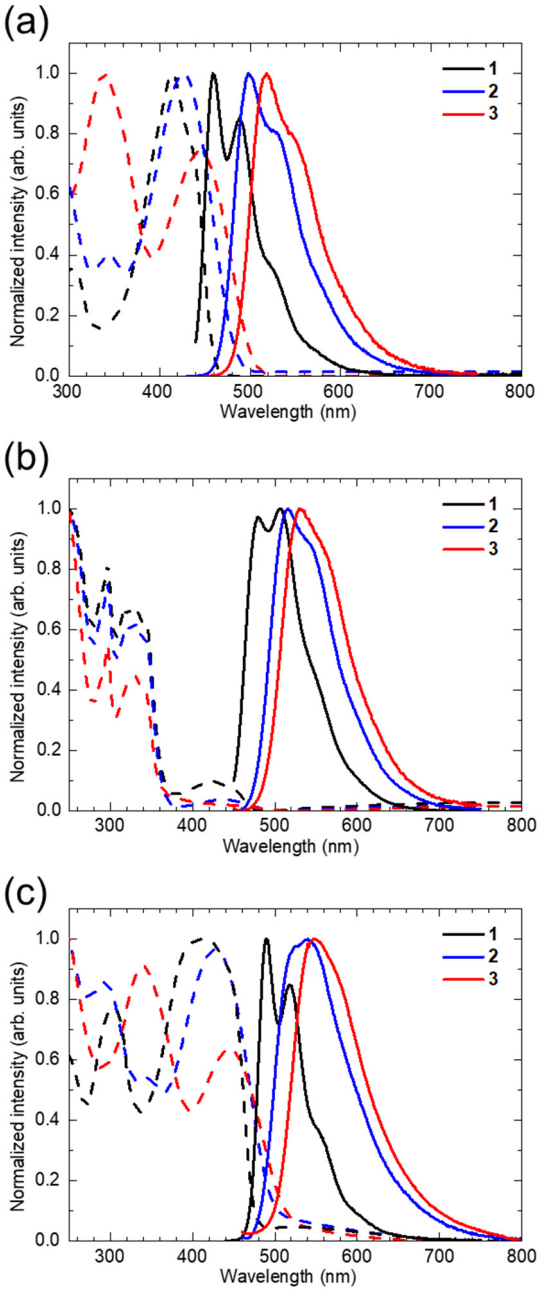

Fig. 2 UV-Vis absorption (dashed lines) and emission (solid lines) spectra of **1**, **2** and **3** (a) in toluene (b) in 6 wt%-doped films of CBP, and (c) in neat films.

Table 1: Photophysical, electrochemical and ASE properties of **1**, **2** and **3** in solution, doped CBP films and neat films.

Compd.	Condition	λ_{abs} [nm]	λ_{PL} [nm]	Φ_{PL} [-][a)]	τ [ns][b)]	k_r / 10^8 [s^{-1}]	HOMO [eV][c)]	LUMO [eV][c)]	E_{th}^{ASE} [μJ cm^{-2}]	λ_{ASE} [nm]
1	In solution[d)]	304, 414	460, 488	0.89	1.3	6.9	−5.02	−2.32	–	–
1	In CBP film[e)]	342, 423	480, 506	0.75	1.2	6.1	–	–	0.85	510
1	In neat film	303, 412	490, 518	0.31	1.3	2.4	−5.61	–	1.6	518
2	In solution[d)]	345, 426	499, 527	0.92	1.4	6.8	−5.06	−2.50	–	–
2	In CBP film[e)]	342, 438	516, 537	0.91	1.3	7.1	–	–	0.89	538
2	In neat film	294, 428	540	0.56	1.4	4.0	−5.63	–	1.6	548
3	In solution[d)]	338, 445	519, 546	0.73	2.0	3.6	−5.01	−2.50	–	–
3	In CBP film[e)]	344, 449	531, 554	0.73	1.3	5.4	–	–	1.2	554
3	In neat film	341, 443	547	0.27	1.4	1.9	−5.61	–	3.2	567

[a)]Absolute PL quantum yield evaluated using an integrating sphere in N_2. [b)]In N_2. [c)]Estimated versus the vacuum level from $E_{HOMO} = -4.80 - E_{ox}$ (vs Fc/Fc^+) or $E_{LUMO} = -4.80 - E_{red}$ (vs Fc/Fc^+) for DCM and ionization potential for neat films measured by photoelectron yield spectroscopy with a Riken Keiki AC-3 apparatus. [d)]Photophysical properties in toluene and HOMO-LUMO levels in DCM. [e)]Absorption maxima of a CBP neat film are at 297, 331, and 343 nm.

that the naphthalene units can contribute to the suppression of the concentration quenching, probably due to the reducing intermolecular interactions in **2**. The k_r of 7×10^8 and 4×10^8 s^{-1} for **2** in the doped and neat films, respectively, are comparable to 8×10^8 and 4×10^8 s^{-1} for the corresponding BSBCz films, respectively. In particular, the optical properties in the neat condition are outstanding in contrast to the conventional green emitters such as coumarin dyes showing strong aggregation caused quenching.[8] These results indicated that the naphthalene unit is useful to improve the optical properties of laser dyes. Further, the optical properties of compound **3** are sufficiently good as green to yellow lasers while the ASE threshold was slightly high compared with that of compound **2** (vide infra). Overall, these compounds showed considerably low ASE thresholds even in the neat films.

Film morphology in the neat films is also important for the waveguide of light. The out-of-plane X-ray diffraction (XRD), atomic force microscopy (AFM), and molecular orientation predicted by variable angle spectroscopic ellipsometry and uniaxial anisotropic models for the neat films are shown in the supporting information (Figs. S6–S8 and Table S3). All of the compounds did not show any peaks in the XRD, indicating amorphous nature of the neat films of **1**, **2** and **3**.The AFM images showed a smooth surface with the root mean square (RMS) roughness of <1 nm for all films. These films showed random molecular orientations with horizontal orientation parameters *S* of −0.04, −0.06 and −0.08 for **1**, **2** and **3** respectively (Table S3).[22] Note that the *S* is generally small for the films fabricated by spin-coating. Differential scanning calorimetry (DSC) showed a clear glass transition temperature at 90.7, 127.8 and 122.0 °C for **1**, **2** and **3**, respectively (Fig. S9), indicating the formation of thermally stable amorphous films.

Fig. 3 shows the emission intensity changes as a function of the irradiation time for the neat films of **1**, **2** and **3** under nitrogen atmosphere. The decay of the PL intensity of **2** is smaller than that of **1**. Thus, the introduction of the naphthalene units can also contribute to improve the photo-stability. In our previous work, it is clarified that the double bond in the stilbene units causes the initial degradation of molecules.[21] Stilbene derivatives are known to undergo *cis-trans* isomerization through triplet excited states upon photoexcitation, which means weakening of double bond and forming of an intermediate with bond twisting 90°.[23,24] Therefore, this transition state may lead side reactions such as oxidation, dimerization, and so on. On the other hand, the isomerization from *trans* to *cis*-conformations is suppressed for

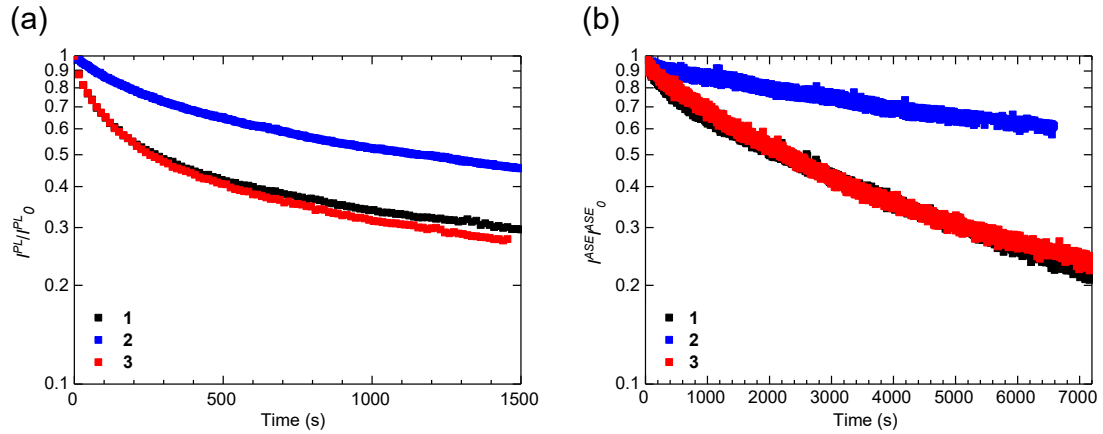

Fig. 3 (a) PL and (b) ASE intensities normalized to the initial as a function of time for **1**, **2** and **3**, irradiated by continuous-wave laser light at 355 nm and a nitrogen gas laser at 337 nm, respectively. Excitation intensities: (a) 120 mW cm^{-2} and (b) 280 μJ cm^{-2}.

2 because the excited triplet states are localized in the naphthalene units.[24] As a result, the degradation of **2** is well suppressed, and the photo-stability of **2** was improved more than 3 times compared with that of **1**. On the other hand, the photo-stability of **3** was similar to that of **1** despite the introduction of naphthalene units, which can be attributed to additional double bonds in the enamine moieties. Although we demonstrated the effect of naphthalene substitution on the stability by the direct comparison between phenylene and naphthalene derivatives, the comprehensive absolute stability might still need to be improved. For example, C—N single bond shows low bond dissociation energy (BDE) compared to C—C bond and causes a bond cleavage to generate exciton quenchers and nonradiative recombination sites.[25] The triphenylamine derivatives are unlikely to be robust compared to fused aromatic systems (Fig. S10). Therefore, further modifications on the triphenyl amine structure might remain as another challenge.

Figs. 4 and S11 show the relationship between the excitation intensity and the emission intensity, and ASE spectra for the doped in CBP and the neat films. The E_{th}^{ASE} of **1**, **2** and **3** doped in CBP films were 0.85, 0.89 and 1.2 μJ cm^{-2}, respectively (Table 1). The ASE wavelengths were 510, 538 and 554 nm for **1**, **2** and **3**, respectively, which agreed with the peaks in the stimulated emission cross section (σ_{em}) spectra (Methods S1 and Fig. S12b). The E_{th}^{ASE} of **1** was significantly decreased compared to that of BSB3 in Fig. 1,[13] which seems to be related to the optimization conditions of the films such as the film thickness because of almost the same steady state emission properties with high k_r in these compounds. Importantly, compound **2** showed low ASE threshold at highly pure green region (532 nm for the green primary in the BT.2020 standard).[26] The ASE threshold lower than 1 μJ cm^{-2} is promising for further investigations in OSLDs, and these performances are better than coumarin dyes and one of the best for the green emitting small molecular laser dyes.[27]

The performances in the neat films are also important because the OSLD was fabricated using the neat thin film of BSBCz in order to suppress the exciton quenching processes. However, the laser properties in neat films for green and red emitters are usually inferior to those for blue emitters because stronger donor-acceptor nature for green and red emitter structures leads stronger aggregation-caused quenching. Therefore, there is a very limited number of reports for the ASE from green-emissive neat films. The E_{th}^{ASE} of the neat films are 1.6, 1.6 and 3.2 μJ cm^{-2} for **1**, **2** and **3**, respectively, in the optimized film thicknesses (130–160 nm) (Fig. 4d–f). The ASE wavelengths of **1**, **2** and **3** were 518, 548 and 567 nm, respectively, which also agreed with the σ_{em} peak for neat films (Fig. S12c). Although the σ_{em} values for **2** were slightly higher than those for **1**, the results of E_{th}^{ASE} were comparable between two compounds. This might be related to the confinement factor, and anisotropic extinction coefficients and refractive indices of the films (Fig. S8 and Table S3).[28] Although these E_{th}^{ASE} are slightly higher than those of the reported blue emitters,

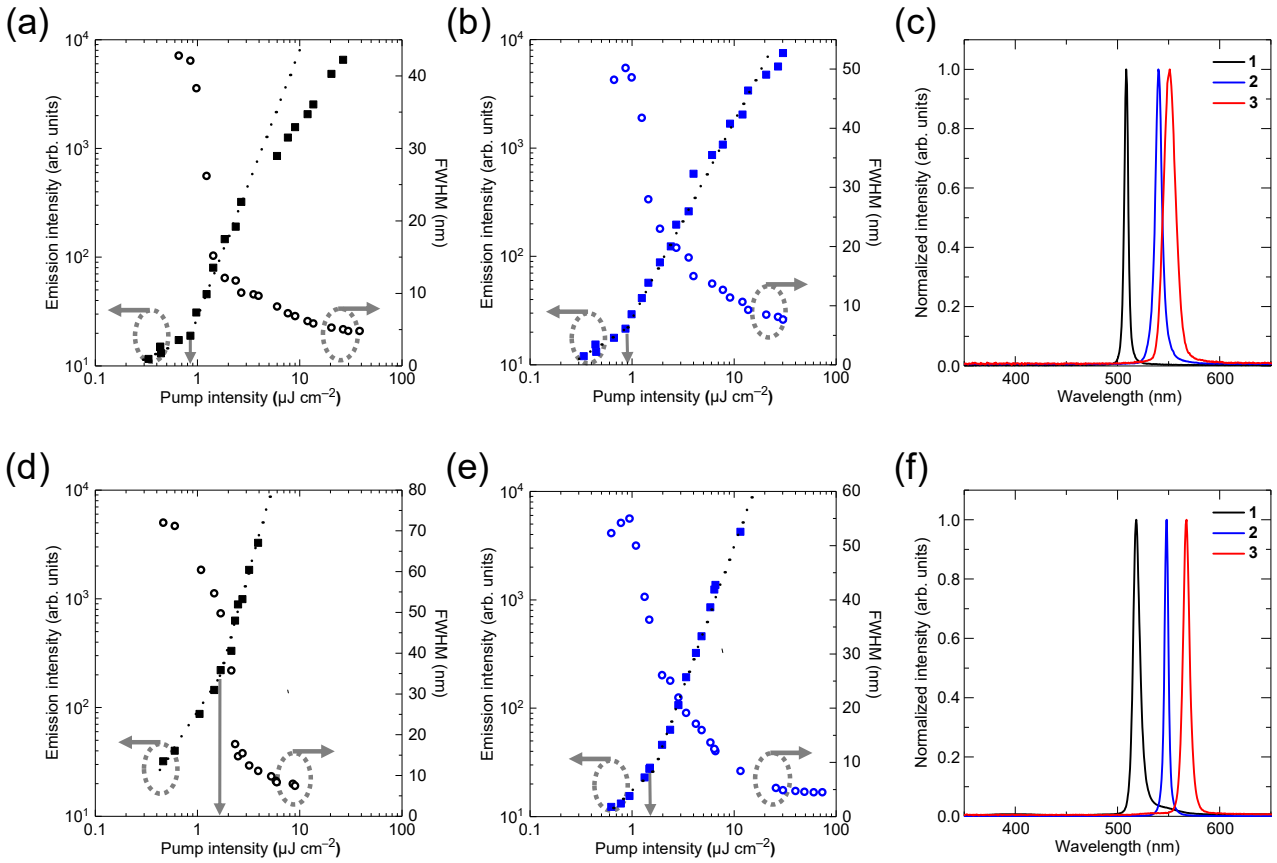

Fig. 4 ASE characteristics. Output PL intensity and full width at half maximum (FWHM) for (a) **1**-doped in CBP and (b) **2**-doped in CBP. (c) ASE spectra of **1**, **2** and **3** doped in CBP films. Output PL intensity and FWHM for neat films of (d) **1** and (e) **2**. (f) ASE spectra of neat films of **1**, **2** and **3**.

these are significantly low compared to previous reports for the green and yellow materials.[29] These low ASE thresholds in the neat films are promising toward improvements of OSLDs. These results clearly demonstrated that the introduction of the naphthalene moiety can easily shift the ASE wavelength to longer wavelength without quenching in the solid state.

4. Conclusions

In this study, diphenylamine-substituted distyrylbenzene derivative was re-investigated with the comparison between benzene and naphthalene moieties. All of compounds **1**–**3** showed low ASE thresholds at the emission wavelengths from green to yellow. In particular, **2** showed one of the best ASE thresholds for the green emitters in the neat condition. This can be attributed to the effect of naphthalene unit affording the red-shift of emission with the suppression of the concentration quenching. The results of photo-degradation test also revealed better photo-stability for the naphthalene derivatives, probably due to the controls of excited state dynamics. Since naphthalene and some π-extended aromatic rings can easily be incorporated, this work introduces a very useful molecular design guideline toward realizing OSLD in green and yellow region.

Conflicts of interest

There are no conflicts to declare.

Acknowledgements

We thank Ms. K. Kusuhara and Ms. N. Nakamura for the characterization of materials. This work was financially supported by JST ERATO Grant Number JPMJER1305, JSPS KAKENHI Grant Number 19H02790 and 20K21227, The Murata Science Foundation, and the JSPS Core-to-Core Program.

Notes and references

1 A. S. D. Sandanayaka, T. Matsushima, F. Bencheikh, S. Terakawa, W. J. Potscavage, C. Qin, T. Fujihara, K. Goushi, J.-C. Ribierre and C. Adachi, *Appl. Phys. Express*, 2019, **12**, 061010.

2 C. W. Tang and S. A. VanSlyke, *Appl. Phys. Lett.*, 1987, **51**, 913.

3 (a) L. Xiao, Z. Chen, B. Qu, J. Luo, S. Kong, Q. Gong and J. Kido, *Adv. Mater.*, 2011, **23**, 926; (b) M. Y. Wong and E. Zysman-Colman, *Adv. Mater.*, 2017, **29**, 1605444.

4 (a) F. P. Schäfer, W. Schmidt and J. Volze, *Appl. Phys. Lett.*, 1966, **9**, 306; (b) I. D. W. Samuel and G. A. Turnbull, *Chem. Rev.*, 2007, **107**, 1272; (c) A. J. C. Kuehne and M. C. Gather, *Chem. Rev.*, 2016, **116**, 12823.

5 A. Otomo, S. Yokoyama, T. Nakahama and S. Mashiko, *Appl. Phys. Lett.*, 2000, **77**, 3881.

6 (a) C. Mowatt, S. M. Morris, M. H. Song, T. D. Wilkinson, R. H. Friend and H. J. Coles, *J. Appl. Phys.*, 2010, **107**, 043101; (b) Y. Kage, S. Kang, S. Mori, M. Mamada, C. Adachi, D. Kim, H. Furuta and S. Shimizu, *Chem. Eur. J.* 2021, DOI: 10.1002/chem.202005360.

7 V. G. Kozlov, V. Bulović, P. E. Burrows and S. R. Forrest, *Nature*, 1997, **389**, 362.

8 H. Nakanotani, T. Furukawa and C. Adachi, *Adv. Opt. Mater.*, 2015, **3**, 1381.

9 H. Nakanotani, T. Furukawa, T. Hosokai, T. Hatakeyama and C. Adachi, *Adv. Optical Mater.*, 2017, 1700051.

10 (a) W. Zhang, Y. Yan, J. Gu, J. Yao and Y. S. Zhao, *Angew. Chem. Int. Ed.*, 2015, **54**, 7125; (b) X. Cheng, K. Wang, S. Huang, H. Zhang, H. Zhang and Y. Wang, *Angew. Chem. Int. Ed.*, 2015, **54**, 8369; (c) V. T. N. Mai, A. Shukla, M. Mamada, S. Maedera, P. E. Shaw, J. Sobus, I. Allison, C. Adachi, E. B. Namdas and S.-C. Lo, *ACS Photonics*, 2018, **5**, 4447.

11 (a) T. Oyamada, C.-H. Chang, T.-C. Chao, F.-C. Fang, C.-C. Wu, K.-T. Wong, H. Sasabe and C. Adachi, *J. Phys. Chem. C*, 2007, **111**, 108; (b) D.-H. Kim, A. S. D. Sandanayaka, L. Zhao, D. Pitrat, J. C. Mulatier, T. Matsushima, C. Andraud, J.-C. Ribierre and C. Adachi, *Appl. Phys. Lett.*, 2017, **110**, 023303.

12 (a) S. Z. Bisri, T. Takenobu, Y. Yomogida, H. Shimotani, T. Yamao, S. Hotta and Y. Iwasa, *Adv. Funct. Mater.*, 2009, **19**, 1728; (b) M. Ichikawa, K. Nakamura, M. Inoue, H. Mishima, T. Haritani, R. Hibino, T. Koyama and Y. Taniguchi, *Appl. Phys. Lett.*, 2005, **87**, 221113; (c) T. Komori, H. Nakanotani, T. Yasuda and C. Adachi, *J. Mater. Chem. C*, 2014, **2**, 4918.

13 T. Aimono, Y. Kawamura, K. Goushi, H. Yamamoto, H. Sasabe and C. Adachi, *Appl. Phys. Lett.*, 2005, **86**, 071110.

14 (a) H. Nakanotani, M. Saito, H. Nakamura and C. Adachi, *Appl. Phys. Lett.*, 2009, **95**, 033308; (b) H. Nakanotani, S. Akiyama, D. Ohnishi, M. Moriwake, M. Yahiro, T. Yoshihara, S. Tobita and C. Adachi, *Adv. Funct. Mater.*, 2007, **17**, 2328; (c) M. Mamada, T. Fukunaga, F. Bencheikh, A. S. D. Sandanayaka and C. Adachi, *Adv. Funct. Mater.*, 2018, 1802130; (d) V. T. N. Mai, A. Shukla, A. M. C. Senevirathne, I. Allison, H. Lim, R. J. Lepage, S. K. M. McGregor, M. Wood, T. Matsushima, E. G. Moore, E. H. Krenske, A. S. D. Sandanayaka, C. Adachi, E. B. Namdas and S.-C. Lo, *Adv. Opt. Mater.* 2020, **8**, 2001234.

15 (a) B. K. Yap, R. Xia, M. Campoy-Quiles, P. N. Stavrinou and D. D. C. Bradley, *Nat. Mater.*, 2008, **7**, 376; (b) C. Karnutsch, C. Pflumm, G. Heliotis, J. C. deMello, D. D. C. Bradley, J. Wang, T. Weimann, V. Haug, C. Gärtner and U. Lemmer, *Appl. Phys. Lett.*, 2007, **90**, 131104.

16 (a) T. W. Lee, O. O. Park, D. H. Choi, H. N. Cho and Y. C. Kim, *Appl. Phys. Lett.*, 2002, **81**, 424; (b) A. Rose, Z. G. Zhu, C. F. Madigan, T. M. Swager and V. Bulovic, *Nature*, 2005, **434**, 876; (c) D. Amarasinghe, A. Ruseckas, A. E. Vasdekis, M. Goossens, G. A. Turnbull and I. D. W. Samuel, *Appl. Phys. Lett.*, 2006, **89**, 201119; (d) A. K. Sheridan, G. A. Turnbull, A. N. Safonov and I. D. W. Samuel, *Phys. Rev.*, **B 62**, R11929.

17 (a) D. Amarasinghe, A. Ruseckas, A. E. Vasdekis, G. A. Turnbull and I. D. W. Samuel, *Adv. Mater.*, 2009, **21**, 107; (b) M. Mamada, R. Komatsu and C. Adachi, *ACS Appl. Mater., Interfaces*, 2020, **12**, 28383.

18 (a) C. Hosokawa, H. Higashi, H. Nakamura, and T. Kusumoto, *Appl. Phys. Lett.*, 1995, **67**, 3853; (b) H. Yamamoto, H. Kasajima, W. Yokoyama, H. Sasabe and C. Adachia, *Appl. Phys. Lett.*, 2005, **86**, 083502.

19 L. E. Contois and L. J. Rossi, (Eastman Kodak Company) US patent publication number US3873312A, 1975.

20 (a) Y. Wang, T. Liu, L. Bu, J. Li, C. Yang, X. Li, Y. Tao and W. Yang, *J. Phys. Chem. C*, 2012, **116**, 15576; (b) B. Xu, H. Fang, Y. Dong, F. Chen, Q. Chen, H. Sun and W. Tian, *New J. Chem.*, 2010, **34**, 1838.

21 Y. Oyama, M. Mamada, A. Shukla, E. G. Moore, S.-C. Lo, E. B. Namdas and C. Adachi, *ACS Mater. Lett.*, 2020, **2**, 161.

22 (a) J. M. Winfield, C. L. Donley and J.-S. Kim, *J. Appl. Phys.*, 2007, **102**, 063505; (b) D. Yokoyama, Y. Setoguchi, A. Sakaguchi, M. Suzuki and C. Adachi, *Adv. Funct. Mater.*, 2010, **20**, 386; (c) T. Komino, H. Nomura, M. Yahiro, K. Endo and C. Adachi, *J. Phys. Chem. C*, 2011, **115**, 19890.

23 (a) J. Saltiel and Y.-P. Sun, In Photochromism. Molecules and Systems; H. Durr, H. Bouas-Laurent, Eds; Elsevier: Amsterdam, 1990; (b) T. Arai and K. Tokumaru, *Chem. Rev.*, 1993, **93**, 23.
24 I. Anger, M. Sundahl, O. Wennerström, K. Sandros, T. Arai and K. Tokumaru, *J. Phys. Chem.*, 1992, **96**, 7027.
25 (a) D. Y. Kondakov, W. C. Lenhart and W. F. Nichols, *J. Appl. Phys.*, 2007, **101**, 024512; (b) D. Y. Kondakov, *J. Appl. Phys.*, 2008, **104**, 084520; (c) A. S. D. Sandanayaka, T. Matsushima and C. Adachi, *J. Phys. Chem. C*, 2015, **119**, 23845.
26 ITU-R Recommendation BT.2020 (2015).
27 H. Nakanotani, T. Furukawa and C. Adachi, *Adv. Opt. Mater.*, 2015, **3**, 1381.
28 T. Komino, H. Nomura, M. Yahiro, K. Endo, C. Adachi, *J. Phys. Chem. C* 2011, **115**, 19890
29 X. Tang, Y.-T. Lee, Z. Feng, S. Y. Ko, J. W. Wu, V. Placide, J.-C. Ribierre, A. D'Aléo and C. Adachi, *ACS Mater. Lett.*, 2020, **2**, 1567.